World Journal of Microbiology and Biotechnology (2019) 35:169
https://doi.org/10.1007/s11274-019-2735-5

ORIGINAL PAPER

Structural and functional evaluation of recombinant histidine phosphokinase NisK and response regulator NisR: in silico and experimental approach

Sahar Heidari[1] · Javad Hamedi[2] · Gholamreza Olad[1] · Jafar Amani[3] · Mona Rastegar Shariat Panahi[4] · Ali Najafi[5]

Received: 27 February 2019 / Accepted: 26 September 2019

Abstract

In the two-component system of NisRK from *Lactococcus lactis*, the production of nisin is affected by transmembrane NisK and activation of intracellular NisR. The transcription of nisin structural genes can be induced by derivatives of nisin. NisR activation leads to the activation of *nisA/Z* transcription, which encodes the nisin maturation machinery, nisin regulation and activation of the nisFEG operon to confer immunity. The aim of this study was to express the *Lactococcus lactis* histidine phosphokinase NisK and response regulator NisR in *E. coli*, and to perform activity assays and in silico analysis. In silico methods were applied to study the properties and structures of the NisK and NisR proteins, including prediction of physicochemical characteristics, secondary and tertiary structure, stability and ligand-receptor interactions.pET32a and pET28a vectors containing synthetic *nisK* and *nisR* genes were transformed into *E. coli* followed by IPTG induction. SDS-PAGE and western blotting methods were applied to confirm the presence and identity of the amplified proteins. Following purification, the proteins were dialyzed and then prepared for activity assay. The CAI index showed that the genes was compatible with the *E. coli* host and that the proteins have effective expression. Also, the mRNA prediction results suggest that there is enough mRNA stability for efficient translation in the new host. NisK and NisR recombinant proteins were expressed in *E. coli* with half - lives of around 10 h and were confirmed with molecular weights of 27 kDa and 69 kDa, respectively, by SDS-PAGE and western blotting. The secondary structure of the recombinant proteins as predicted by circular dichroism spectroscopy was similar to the in silico protein structures. Activity assay of recombinant NisK was performed by measuring the amount of consumed ATP according to the light produced by luciferase. Because NisK and NisR have a direct impact on each other, they have an essential role in increasing the production of nisin and they can be used in different research fields. Our results demonstrated that recombinant proteins NisK and NisR preserved their structure and function after expression.

Keywords *E. coli* · Histidine phosphokinase NisK · Nisin · Recombinant protein · Response regulator NisR

Electronic supplementary material The online version of this article (https://doi.org/10.1007/s11274-019-2735-5) contains supplementary material, which is available to authorized users.

✉ Gholamreza Olad
grolad@gmail.com

✉ Jafar Amani
jafar.amani@gmail.com

[1] Applied Biotechnology Research Center, Baqiyatallah University of Medical Sciences, Vanak Sq. Molasadra St., P.O. Box 19395-5487, Tehran, Iran

[2] Department of Microbial Biotechnology, School of Biology, College of Science, University of Tehran, Tehran, Iran

[3] Applied Microbiology Research Center, Systems Biology and Poisonings Institute, Baqiyatallah University of Medical Sciences, Vanak Sq. Molasadra St., P.O. Box 19395-5487, Tehran, Iran

[4] Department of Biochemistry, Payame Noor University, Tehran, Iran

[5] Molecular Biology Research Center, Baqiyatallah University of Medical Sciences, Tehran, Iran

Published online: 25 October 2019

Introduction

The most significant lantibiotic produced by *Lactococcus lactis* is a 34-amino acid peptide called nisin. This peptide contains dehydro residues and owns five lanthionine ring structures (Chatterjee et al. 2005; Zhang et al. 2012) and also has broad usage as a safe and natural food preservative (Gharsallaoui et al. 2016). Therapeutic applications of nisin include therapy of clinical bovine mastitis, prevention of head and neck cancer tumorigenesis, and oral and dental treatment along with other treatments (Wu et al. 2007; Field et al. 2015; Kamarajan et al. 2015).

A gene cluster consisting of 11 genes (*nisABTCIPRKFEG*) is associated with nisin biosynthesis. Pre-nisin contains serine and threonine residues and is encoded *nisA* and then is dehydrated to dehydroalanine and dehydrobutyrine via NisB and thioether bridges are formed by NisC cysteines cyclization. NisT is responsible for transportation of pre-nisin through the cell membrane and protease NisP cleaves the leader peptide, releasing mature nisin. The structure of nisin has been explained as comprising a linear peptide with five intermolecular lanthionine rings and it is a member of the AI lantibiotics group (Chatterjee et al. 2005). The very first discovered bifunctional lantibiotic was nisin which, other than its antimicrobial aspect, operates as a signal via the quorum sensing system NisK/R (two-component regulatory system) in order to induce its biosynthesis (Kuipers et al. 1995).

One of the most common regulatory systems in bacteria, some lower eukaryotes and plants is the two-component system (TCS) (Wuichet et al. 2010; Schaller et al. 2011). The TCS is used by microbes to perceive environmental signals and therefore regulates essential gene expression, enabling them to live in diverse conditions. A cognate response regulator (RR) and a Histidin phosphokinase (HPK) are the components of the TCS system (West and Stock 2001). Sensor C is responsible for sensing particular stimuli, followed by auto-phosphorylation on a conservative histidine residue. This leads to activation of the HPK which transfers a phosphate group to its paronymous RR, located on the conservative aspartic acid residue, resulting in the beginning of the downstream gene expression (West and Stock 2001). The C-terminal of the HPK is made up from two conservative domains of which one is responsible for dimerization and its conserved histidine participates in auto phosphorylation. The other conserved domain is the catalytic and ATP binding (CA) domain. The sensor regions are located on N-termini of HPKs, which differ significantly in membrane topology, sequence and structure so that they can recognize different environmental stimuli accurately. The HPKs are categorized into three main types based on sensor location whereby the first and third groups have extracellular and cytoplasmic sensor domain, respectively, and the second group contains multiple transmembrane helices that are connected to the sensing regions (Mascher et al. 2006).

Currently, thousands of TCS components have been discovered, while the majority of the studies are appertained to conserved cytoplasmic regions due to the complications of expression and structural survey of membrane proteins. The study of the first group of HPKs and their extracellular domains showed that they include a mixture of alpha–beta folds (displayed by PDC domain), alpha folds (displayed by NarX sensor domain), and sensor domains which adopt a similar fold to extracellular binding proteins (displayed by HPK29s) (Cheung and Hendrickson 2010). HPKs can mostly be seen in gram-negative bacteria and their correlated ligands are mostly ions or small molecules (Reinelt et al. 2003; Cheung and Hendrickson 2010). Gram-positive bacteria generally recognize peptides as quorum sensing pheromones in order to activate TCS or other regulatory cascades to regulate biosynthesis or different cellular processes (Mascher et al. 2006).

In this study, we manipulate the NisK and NisR genes for recombinant protein production, and investigate the structural and functional characteristics of the recombinant proteins.

Material and methods

Bacterial strains, plasmids and media

E. coli BL21(DE3), E. coli DH5α (ATCC 35,218) and *E. coli Rosetta-gami (DE3),* pET28a and pET32a, and BamHI and XhoI were used as bacterial strains, expression vectors, and restriction enzymes respectively. *E. coli* DH5α competent cells were produced the calcium chloride ($CaCl_2$) protocol. LB-agar and LB-broth were used as growth media in this study.

Protein retrieval and sequence analysis

The sequences of the NisK and NisR proteins were obtained from the UniProt knowledge database with accession numbers P42707 and Q07597, respectively. Sequence alignments were done using the website of the National Centre for Biotechnology Information (NCBI) (https://blast.ncbi.nlm.nih.gov/Blast.cgi in FASTA format). Evolutionary analyses were conducted in MEGA X.

Gene optimization and mRNA structure prediction

Sequences of the target proteins NisK and NisR were translated into DNA sequences (https://www.bioinformatics.

org/sms2/rev_trans.html) and by applying gene optimization software (https://www.dna20.com/resources/genedesigner), genes were optimized for proper expression in *E. coli* (Grote et al. 2005). The genes were synthesized by General Biosystems, Inc. (USA).

The mRNA secondary structure of genes was analyzed by bioinformatics tools including the mfold program at https://www.bioinfo.rpi.edu/applications/mfold (Zuker 2003).

Protein characterization

By using the ExPASy program ProtParam (https://web.expasy.org/protparam), the general characteristics of proteins, namely aliphatic and instability index, half-life of proteins, molecular weight, negative and positive residues, grand average hydropathy (GRAVY), isoelectiric point (pI) and extinction coefficient were extracted (Gasteiger et al. 2005).

Secondary and tertiary structure prediction and analysis

The Garnier-Osguthorpe-Robson secondary structure prediction version IV was applied to compute and analyze the secondary structural features of NisK and NisR proteins (Garnier et al. 1996). The I-TASSER online server was used in order to obtain the 3D structure of the recombinant proteins by using confidence score (C-score) (Zhang 2008).

Predicted topologies

Because NisK is a membrane protein its membrane topology was analysed using the online server TMHMM (https://www.cbs.dtu.dk/services/TMHMM/) (Möller et al. 2001), for which the results will be described and discussed subsequently.

Transformation and expression of proteins

The recombinant pET28a and pET32a plasmids were transformed into *E. coli* DH5α competent cells. Cells were cultured on LB-Agar containing 50 µg/ml kanamycin for pET28a and 50 µg/ml ampicillin for pET32a and incubated overnight (18 h) at 37 °C. Plasmid extraction was done by Hybrid-QTM Plasmid Rapidprep Kit® (Gene All®). The extracted plasmids were confirmed by gel electrophoresis. BamHI and XhoI restriction enzymes were used for gene confirmation for use in the transformation process. The recombinant constructs (pET32a-nisK and pET28a-nisR) were transformed into *E. coli* Rosetta and *E. coli* BL21 competent cells, respectively. The transformed bacteria were cultured in 500 ml LB broth medium supplemented with kanamycin and ampicillin (50 µg/ml) at 37 °C. The culture for NisK was induced by addition of isopropyl β-D-1-thiogalactopyranoside (IPTG) at a final concentration of 1 mmol/L (OD600 between 0.6–0.8) and then incubated for 7 h at 37 °C. The culture for NisR was induced by 0.5 mmol/L IPTG then incubated overnight (18 h) at 25 °C.

Cells were collected by centrifugation and then lysed using 50 mM Tris–HCl buffer (1.5 ml, pH 8.0) along with 10 mM PBS buffer (pH 7.4) or 150 mM NaCl. The samples were sonicated 3 times with 30-second bursts and 30 s on the ice between intervals and after lysing by sonication, cells were centrifuged at 14,000 rpm for 30 min to remove intact cells. The supernatant was ultra-centrifuged at 12,000 rpm for 2 h to separate soluble (cytoplasmic fraction) and insoluble (cell membrane fraction) proteins. Following this procedure, pellets were suspended in buffer (8 M Urea, 50 mM NaH_2PO_4, 50 mMTris-HCl) and were shaken at room temperature for 1 h. The samples were then centrifuged at 10,000 rpm for 30 min followed by evaluation on SDS-PAGE (10% polyacrylamide gel) (Sambrook et al. 1989).

Protein purification

A Ni–NTA agarose column (QIAGEN Inc., USA) was used in order to purify the His-tagged proteins. Lysis buffer (8 M Urea, 0.1 M NaH2PO4, 0.01 M Tris·Cl, 0.05% Tween 20, pH 8.0) was applied to suspend the pellets which were obtained from centrifugation of cell lysate at 14000 rpm for 30 min, followed by shaking for 1 h at room temperature. The supernatant was applied to Ni–NTA resins. Washing buffer (8 M Urea, 0.1 M NaH2PO4, 0.01 M Tris·Cl, 0.05%, imidazole 20 mM) was used for washing the resin 3 times after 2 h of incubation of supernatant with resin. Finally, the elution buffer (8 M Urea, 0.1 M NaH2PO4, 0.01 M Tris·Cl, 0.05%, imidazole 250 mM) was used to elute the recombinant protein. A decreasing gradient of urea concentration was dialyzed against the proteins to eliminate the urea from the solvent. Protein concentration was estimated by Bradford assay and the total amount of purified and dialyzed soluble protein was determined. Purified proteins were also analyzed by SDS-PAGE.

Western blotting

Following SDS-PAGE, the purified proteins were transferred to a PVDF membrane (Roche, Germany) along with transfer buffer (120 mM glycine, 15.6 mM Tris-base and 20% methanol). 5% skimmed milk (5 g skim milk powder in 100 ml 1 × PBS) was used as the blocking agent on the membrane (1 h at 37 °C) in order to block nonspecific antibody binding. After washing the PVDF membrane with PBS-T (PBS + 0.05 tween 20), it was incubated in anti rabbit His-Tag conjugated HPR (Sigma) polycolonal antibody with a dilution of 1:2000 in the 1 × PBS buffer with gentle shaking for 1 h at 37 °C. The detection of proteins was done using

3,3-diaminobenzidin (DAB) as the substrate and also hydrogen peroxide in order to remove fixed antibodies.

Circular dichroism (CD) measurements

The secondary structure content of the purified recombinant proteins was analysed by far-UV circular dichroism spectroscopy.

CD spectra were obtained on a JASCO J-810 CD spectrometer (Tokyo, Japan) using solutions with protein concentration of at least 0.2 mg/ml, at room temperature using a 0.1 cm quartz cell at a scan rate of 100 nm/min. Each protein sample with concentration of 400 mg/l was mixed with 50 ml of Tris buffer (pH 8) and this buffer was also used as the blank (Tafreshi et al. 2008). The CD spectrum of the cuvette containing dialysis buffer was recorded and subtracted from the same solution containing the proteins.

Ligand-receptor docking

The docking process consists of two major steps: ligand conformation prediction and its orientation status (known as pose) and also evaluation of the binding affinity. More negative the e- value more efficient is the docking. The Z-dock server was used to perform docking. This server calculated protein–ligand interactions and investigated the application of the models for ligand binding potency prediction.

Enzyme activity assay

An ATP standard curve consisting of a dilution series was created and several statistical parameters were calculated from the obtained data. The estimation of kinetic rate constant for ATP was performed using a range of concentrations: 40 ml of ATP (0.004–8 mM) was mixed with assay reagents consisting of 10 mM Tris, 1 mM Luciferase, and 5 mM MgSO4. The reaction was initiated by adding 10 ml of enzyme and light emission was recorded over 10 s. The ATP content was defined according to the standard curve.

One of the most sensitive analytical tools in order to measure the consumption of the ATP in NisK assay is monitoring the low production of luciferase. In this method, a substrate solution containing 5µL of NisK recombinant protein, 5µL of 40 mM ATP and 5µL of substrate (NisR) was used and was incubated for 5 min. Following the incubation, 5 µL of enzyme was added to the reaction buffer consisting of 10 µl of 50 mM ATP free complex, 10 mM Tris buffer, 1 mM Luciferase, 5 mM MgSo4 and light emission was recorded over 10 s (Sirius tube luminometer, Berthold Detection System, Germany). The measured protein concentration was 400 mg/l approximately. 50 mM Tris buffer was used as a blank instead of protein (Mortazavi and Hossein khani 2011).

Results

The in silico analysis using the Codon adaptation Index (CAI) (Dorić et al. 2018) confirmed the efficiency of protein expression as it predicted an index of 0.93 for *nisK* and 0.94 for *nisR* (https://www.genscript.com/tools/rare-codon-analysis). Prediction of mRNA structure and stability of the *nisK* and *nisR* transgenes using the online software mfold demonstrated sufficient stability necessary for efficient translation of the transgenes as indicated in Fig. 1.

The minimum free energy of the secondary structure of proteins formed by RNA was predicted as follows: $\Delta G = -61.05$ kcal/mo for NisR and $\Delta G = -145.38$ kcal/mol for NisK (Table 1).

The *nisK* and *nisR* genes were synthesized and optimized and cloned in vectors pET32a and pET28a, respectively. After transformation of vectors into *E. coli* DH5α and subculturing the selected colonies in LB-broth and plasmid extraction, the extracted plasmids were confirmed by gel electrophoresis. As it can be seen in Fig. 2, the BamHI and XhoI restriction enzymes were applied in gene confirmation and the transformation step.

In silico analysis of NisK and NisR

The NisK protein (UniProt ID: P42707) containing 447 amino acids had a molecular weight of 51,319.63 Da and its theoretical pI was 5.71. The total number of negatively charged residues in NisK was (Asp + Glu) = 56 and the total number of positively charged residues in NisK was (Arg + Lys) = 46. The predicted the half-life of the NisK protein was approximately 30 h (in vitro, mammalian reticulocytes), above 20 h in yeast (in vivo) and higher than 10 h in *E. coli* (in vivo). The instability index (II) was 44.79 and it was classified as an unstable protein.

The NisR protein (UniProt ID: Q07597) containing 229 amino acids had a molecular weight of 26,714.60 Da and its theoretical pI was 5.15. The total number of negatively charged residues of NisRwas (Asp + Glu) = 37 and the total number of positively charged residues in NisR was (Arg + Lys) = 29. The Predicted half-life of NisR protein was approximately 30 h (in vitro, mammalian reticulocytes), above 20 h in yeast (in vivo) and higher than 10 h in *E. coli* (in vivo). The instability index (II) was 54.07 and it was classified as an unstable protein.

The secondary structure of NisK and NisR proteins were predicted by online servers as shown in Fig. 3. The predicted structure contents of the NisK and NisR were identical to our obtained recombinant proteins. The obtained results showed that the structural contents of proteins include extended strand, random coil, and alpha

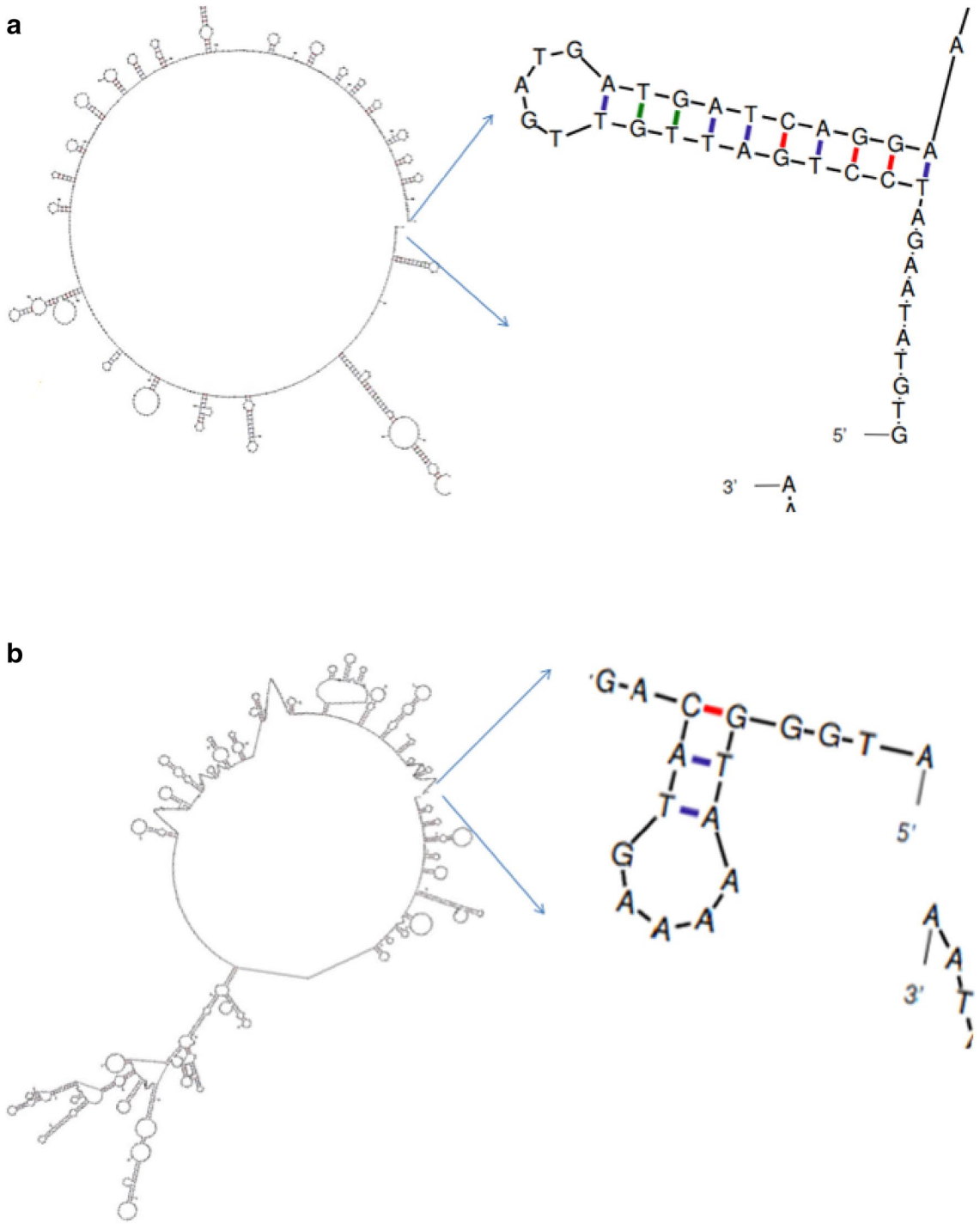

Fig. 1 Prediction of RNA secondary structure of *nisK* (**a**) and *nisR* (**b**) genes by the Mfold server

helix. Additionally, the predicted secondary structure for NisR protein contained 11.84% extended strand, 43.42% alpha helix, and 44.74% random coil and the predicted secondary structure for NisK protein contained 21.48% extended strand, 41.39% alpha helix and 31.14% random coil. The results related to the tertiary structure of the proteins obtained by I-TASSER software (https://zhanglab.ccmb.med.umich.edu/I-TASSER/). In order to determine the tertiary structure of NisK and NisR proteins using TASSER-I server, the FASTA format of these two protein sequences were obtained from UniProt database and were made available to the server. Out of the five models made

Table 1 Free energy details related to 5′ end of *nisK* and *nisR* genes mRNA structure by mfold web server

Structural element	Freeenergy (kcal/mol)	Base pair
nisK		
Stack	− 1.44	External closing pair is G^{5}–C^{15}
Stack	− 0.58	External closing pair is T^{6}–A^{14}
Helix	− 2.02	3 base pairs
Hairpin loop	2.80	Closing pair is A^{7}–T^{13}
nisR		
Stack	− 1.30	External closing pair is T^{11}–A^{35}
Stack	− 1.84	External closing pair is C^{12}–G^{34}
Stack	− 1.28	External closing pair is C^{13}–G^{33}
Stack	− 1.45	External closing pair is T^{14}–A^{32}
Stack	− 1.30	External closing pair is G^{15}–C^{31}
Stack	− 0.88	External closing pair is A^{16}–T^{30}
Stack	0.34	External closing pair is T^{17}–A^{29}
Stack	0.52	External closing pair is T^{18}–G^{28}
Stack	0.07	External closing pair is G^{19}–T^{27}
Helix	− 7.12	10 base pairs
Hairpin loop	2.70	Closing pair is T^{20}–A^{26}

by I-TASSER, model one with the highest C-score was considered as the best model.(Fig. 4).

Predicted topologies

The consensus topology of NisK with low ΔG value showed 1 membrane helices that most of it is inside and other helices more inside (Fig. 5). Membrane topology of NisK by other servers {OCTOPUS server (https://octopus.cbr.su.se/) and TOPCONS (https://topcons.cbr.su.se/)} also showed the same results as TMHMM (data not shown).

Expression, purification and verification of recombinant NisK and NisR proteins

The recombinant proteins with molecular weights of approximately 27 kDa and 64 kDa were expressed after culturing the transformed colonies and inducing with IPTG. The 52 kDa NisK protein was transferred into the pET-32 α (+) vector, fused with the 109 aaTrx·Tag™ thioredoxin protein with a 12 kDa molecular weight that was designed for expression of peptide sequences (Fig. 6 a, b) (Rostami et al. 2016). According to densitometric analysis (Imagej Software) of samples resolved by SDS-PAGE, the proteins were purified to approximately 70% following washing with 3 M urea and to 96% after applying to the Ni–NTA column (Fig. 6 c, d). Based on Bradford assay, the final concentrations of NisK and NisR were 400 µg/ml and 500 µg/ml respectively. The purification yields for NisK was 20 mg/L and for NisR was 25 mg/L respectively.

Western blotting was used to verify that the NisR and NisK proteins had molecular weights of 27 kDa and 64 kDa, respectively (Fig. 7).

Circular dichroism analysis of secondary structure

In order to determine the secondary structure of the protein, CD analysis was performed on the purified protein. The secondary structure estimation software was applied to analyzing the obtained CD data which is mentioned in material and methods section. Table 2 is demonstrating the outcome of the percentage of secondary structure estimation. CD spectra of recombinant proteins shown in Fig. 1 in supplementary. The data obtained from the experiments are compatible with the theoretical predictions.

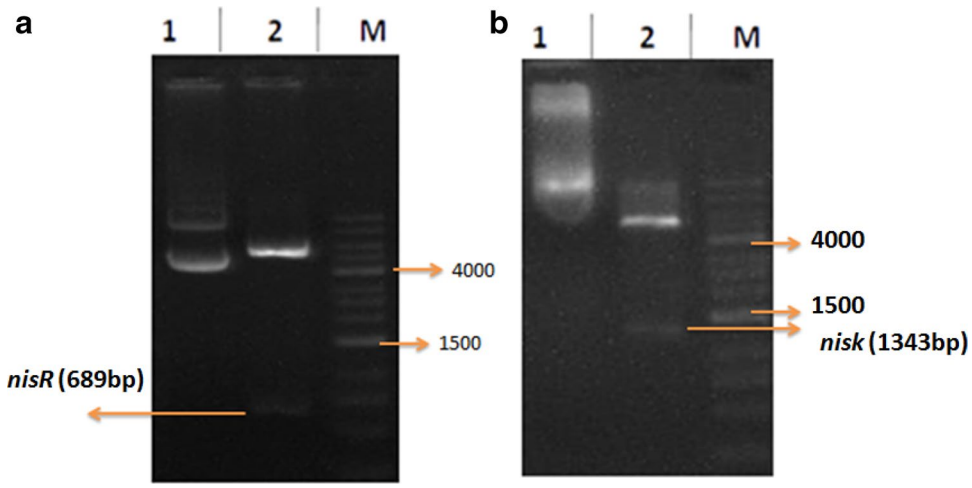

Fig. 2 Restriction digestion confirmation of the *nisK* and *nisR* genes in vectors using enzymes BamHI and XhoI. **a** Lane 1: extracted plasmid, lane 2: plasmid digested with BamHI and XhoI and *nisR* gene (689 bp), *M* DNA marker. **b** Lane 1: extracted plasmid, lane 2: plasmid digested with BamHI and XhoI and *nisk* gene (1343 bp), *M* DNA marker

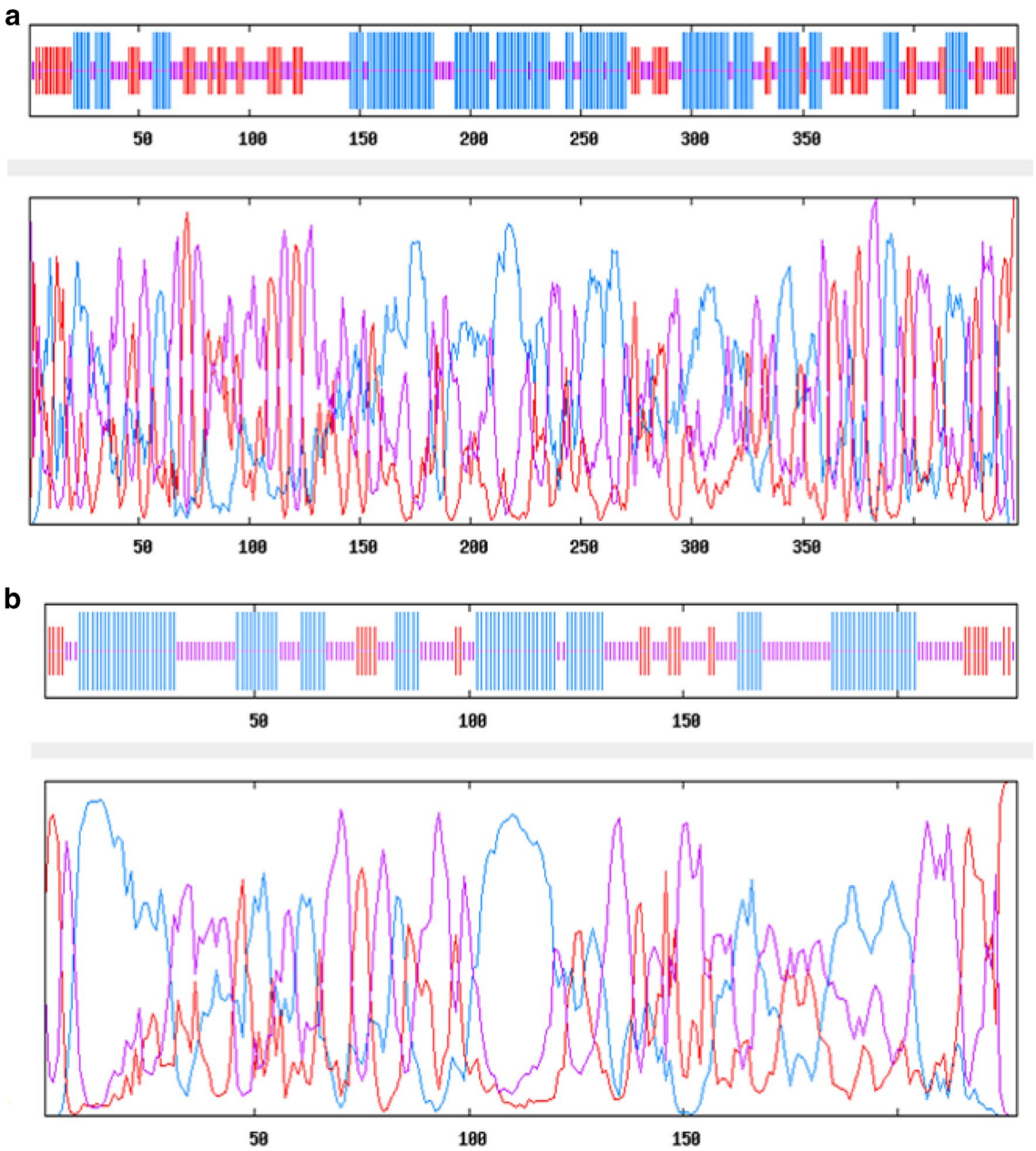

Fig. 3 Graphical results of secondary structure prediction. Red, orange, and blue colors indicate extended strand, coil, and helix, respectively. **a** secondary structure prediction of NisK protein. **b** secondary structure prediction of NisR protein

Ligand docking result

Docking was performed using z-dock software in order to calculate protein–ligand docking. We uploaded a pair of NisK receptor and nisin protein as a ligand structure in PDB format in the z-dock.

The visualization tool Discovery studio 2017 was used to study the docking between the receptors of protein and the ligand, as shown in Fig. 8.

Default parameters were used for carrying out the assay. To be able to analyze the docking, the E-values obtained from z-dock software were applied. The docking process was more efficient, related to the negative E-value.

Analysis of enzyme activity

A standard curve with different ATP concentrations was generated for each series of analysis. The ATP content

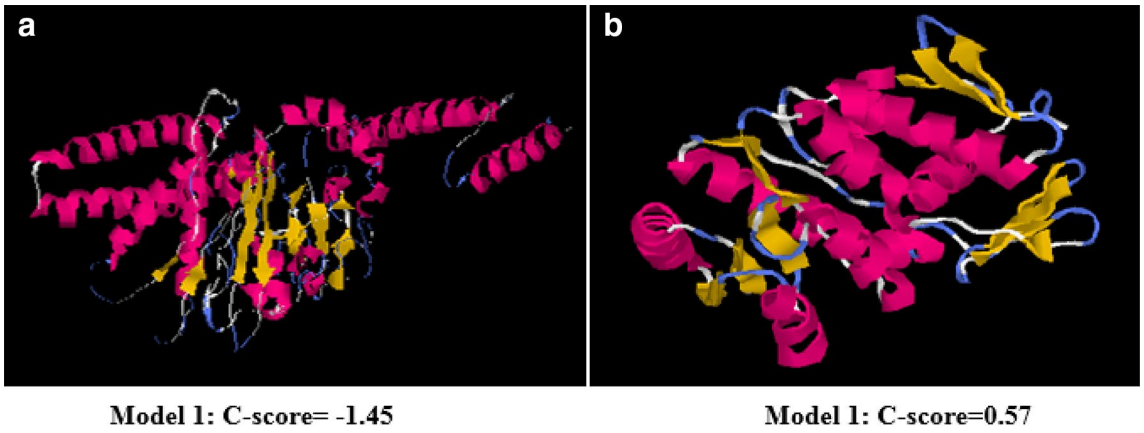

Fig. 4 I-TASSER predictions of tertiary structure. **a** Predicted the tertiary structure of NisK. **b** Predicted tertiary structure of NisR

was determined using the formula of the standard curve (Lineweaver–Burk Plot) (Fig. 9).

To evaluate the effectiveness of the produced histidine phosphokinase recombinant enzyme (NisK) and their substrate, response regulator protein (NisR), ATP consumption was studied through a sensible modification of the luciferase assay. Light output was measured using a conventional liquid-scintillation counter and the protein activity was calculated using the following formulas, and the final results calculated by Excel were as follows:

$$\text{Protein activity} = \frac{\text{Substrate consumption}}{\text{Incubation time}}$$

$$\text{Specific Activity} = \frac{\text{Obtained activity}}{\text{Protein concentration (mg)}}$$

The results are as follows:

Enzyme activity = 56.56 Unit/ml.

Specific enzyme activity = 188.54 Unit/liter.

To measure the performance of the NisK enzyme, we used the Sirius tube luminometer (Berthold Detection System, Germany), which measures the amount of light produced by Luciferase which is one of the analytical and sensitive tools for measuring ATP consumption. Several HPKs are able to act as phosphatases and cause signaling, because HPKs are capable of transferring a phosphoryl group from ATP to a histidine residue, followed by transportation of an aspartate to a RR.

The results in the diagram show that this enzyme has the ability to separate the phosphoryl group, although it is weak (because of the low concentration), indicating proper function of the protein and correct protein folding.

Discussion

Strains of *Lactococcus lactis* subsp. *lactis* are known for their ability to produce nisin, which is an antimicrobial peptide capable of obstructing the growth of Gram-positive and also spores of Clostridia and Bacilli. Nisin has a wide range of usage as a crucial ingredient in industries such as veterinary, pharmaceutical and healthcare. Consequently, many efforts have been made in order to enhance nisin production. The system of transferring the extracellular signals is done by regulating the phosphorylation of a response regulator which starts with transportation of a phosphoryl group by a sensor kinase to a response regulator. Eventually, the phosphoryl group is transferred by the response regulator to a phosphortransferase which contains histidine (Mascher et al. 2006). There is a two-component system which consists of histidine phosphokinase NisK (a transmembrane protein) and NisR (a response regulator). Extracellular nisin autophosphorylates NisK and then NisK transfers the phosphate to NisR. The downstream signal is fortified by phosphorylated NisR via attaching to two regulated promoters which exist in a nisin gene cluster.

The nisin gene cluster has been studied previously in order to increase the expression of nisin. For example, Kim et al. demonstrated that resistance to nisin is increased through introducing the plasmid owning immunogenic genes (*nisI*,*nisFEG*) into the nisin-producing bacterium *Lactococcus lactis* subsp. *lactis* MG1363 causes an enhancement in the production of nisin. They proposed that the concentration of nisin can be affected by NisK and NisR concentration, and also an increase in expression of host immune

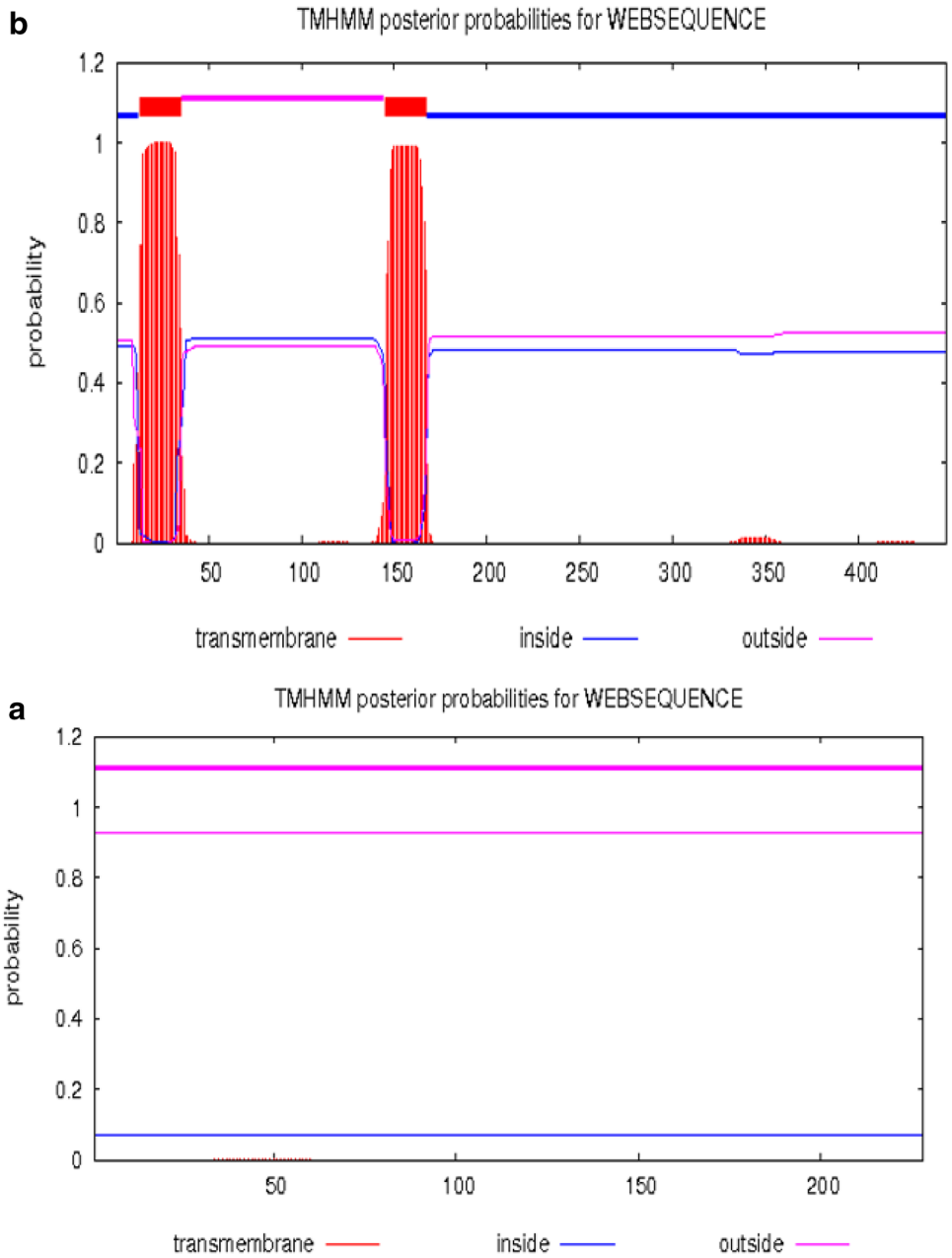

Fig. 5 Predicted membrane topology of NisK and NisR by TMHMM. **a** without any the transmembrane domains. The blue line indicates loops facing inside (cytoplasma), while the pink line depicts loops facing outside (periplasmic space). The numbers at the bottom indicate the amino acid numbers in NisR. **b** The transmembrane domains are shaded in red. The blue line indicates loops facing inside, and the pink line depicts loops facing outside. The numbers at the bottom indicate the amino acid numbers in NisK

genes leads to an increase in the maximum amount of nisin production (Kim et al. 1998).

In food industries (food grade quality), in order to produce proteins, metabolites, and enzymes, a system is widely used which is nisin-controlled expression system (NICE) for *L.lactis* accounts as a self-regulation system for biosynthesis of nisin. As stated earlier, the induction of *nisA* and *nisF* promoters through the NisRK two-component regulatory system is activated by extracellular nisin, which acts as a peptide pheromone (auto-inducer). Consequently, by preparing plasmids owning the *nisA* or *nisF* promoter along with an appropriate cloning site to insert the gene(s) of interest and also a convenient NisRK expressing production host, the production of nisin is done through a controlled expression system which encodes the gene of interest followed by adding the auto-inducer nisin into the growth medium. e-value, aiming to manage the NICE system, the dual plasmid system containing a NisRK expressing plasmid with another plasmid containing nisin-induced nisA promoter was applied. The NICE system is considered as a practical system owing to its diverse advantages over other systems and is used in various LAB hosts in order to obtain biotechnological products and metabolic engineering. The knowledge of the molecular mechanism of nisin and also the characteristics of the nisin biosynthesis regulator is the key factor in potent production and also the optimization of nisin. Generally,

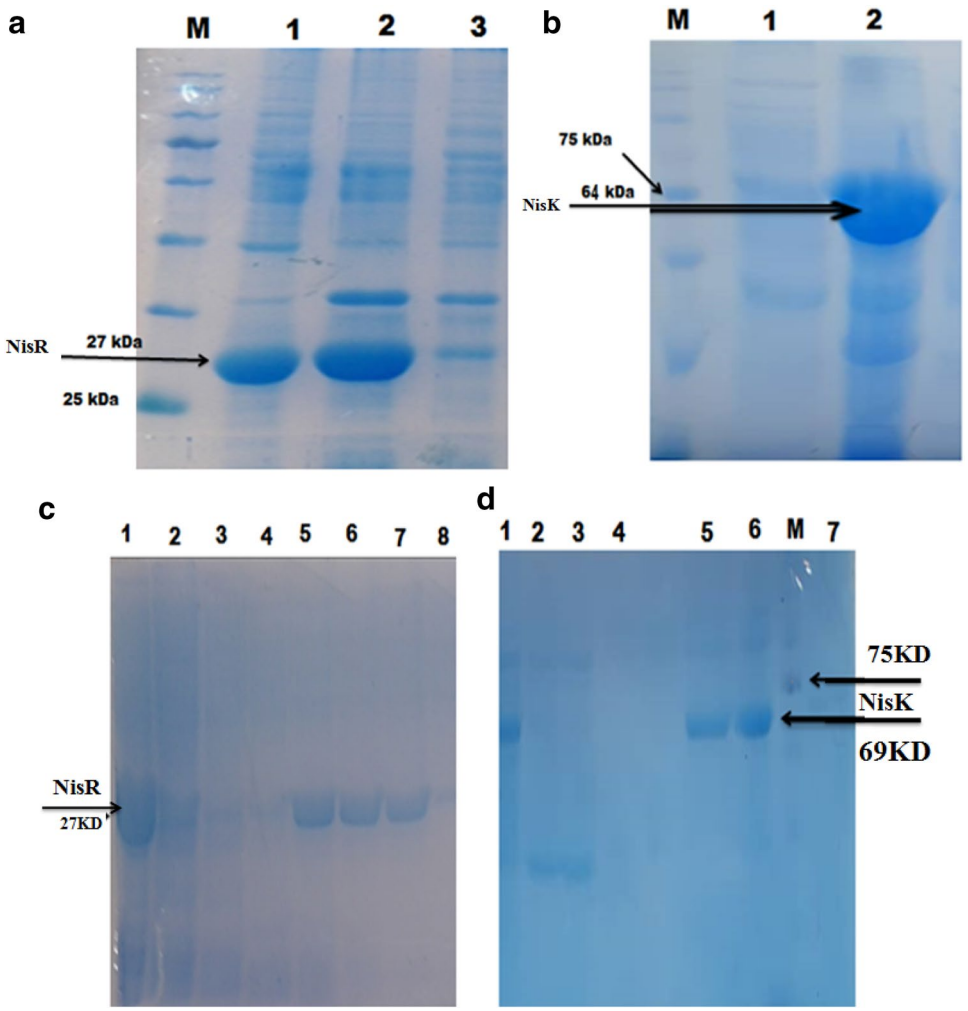

Fig. 6 SDS-PAGE analysis of expressed and purified recombinant proteins. **a** Lane M: Protein marker, lane 1 total soluble protein fraction of NisR (induced 0.5 mM IPTG) *E. coli* BL21, overnight, 25 °C, lane 2 total soluble protein fraction of NisR (induced 1 mM IPTG induced) *E. coli* BL21, 7 h, 37 °C, lane 3 Control sample without IPTG. **b** Lane M: Protein marker, lane 1 Control sample without IPTG, lane 2 total soluble protein fraction of NisK (induced 1 mM IPTG) *E. coli* Rosetta, 7 h, 37 °C. **c** Lane 1 Soluble NisR protein before running on Ni–NTA column, lane 2 flow, lane 3 washing 20, lane 4 washing 60, lane 5 Eluted protein 150, lane 6 Eluted protein 250, lane 7 Eluted protein 500, lane 8 MES buffer d: Lane1 Soluble NisK protein before running on Ni–NTA column, lane 2 flow, lane 3 washing 20, lane 4 washing 60, lane 5 Eluted protein 250, lane 6 Eluted protein 500, lane 7 MES buffer, M: marker

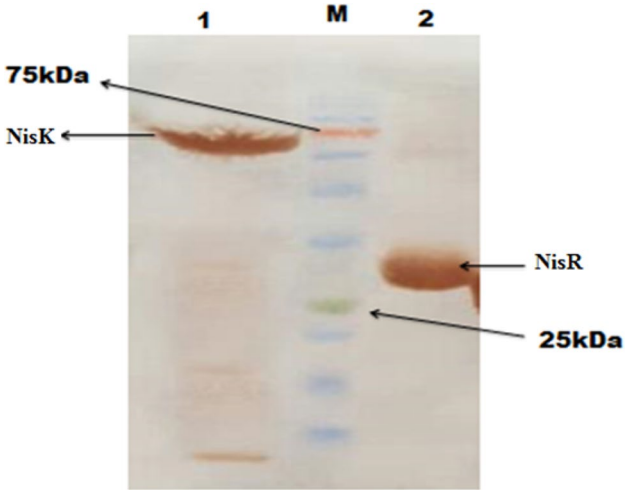

Fig. 7 Western blot analysis of proteins. Lane 1 NisK, lane 2 protein marker, lane 3 NisR

genetic manipulation is one of the main efforts that have been practiced to enhance the production of nisin (Willem, 1996). Lately, improvement of nisinZ production in *Lactococcus lactis* subsp. *Lactis* A164 has been practiced by introducing numerous copies of *nisRK* or *nisFEG* genes (which are involved in nisin biosynthesis) into the A164 strain. The results demonstrated that in the two-component NisKR regulation system, the application of multiple genes variants caused an increase in nisin Z production through enhancement in the transcription of *nisZ* structural gene expression. Moreover, the production of nisin Z increases due to an enhancement in immunity to nisin, perhaps it is because of the decrease in the quantity of nisin in the cell and also an increase in total concentration of nisin. Earlier studies proved that genetic manipulation is able to increase the production of nisin by using strains which can be done through the understanding the basis of nisin biosynthesis procedure and metabolic condition. Hence, the production of nisin can be improved by using these approaches as well as the application of heterologous hosts (Kim et al. 1998).

Table 2 Comparing the percentages of secondary structure of the proteins predicted by bioinformatics tools with data obtained by CD, using the secondary structure estimation software. predicted NisR protein, predicted NisK protein

nisR	Alpha-helix(%)	Beta-strand (%)	Random coil(%)
Predicted NisR protein			
Predict	43.42%	11.84%	44.74%
CD	41.92	11.79	46.29
nisK	Alpha- helix(%)	Beta-strand (%)	Random coil(%)
Predicted NisK protein			
Predict	41.39%	21.48%	37.14%
CD	36.8%	15.00%	48.2%

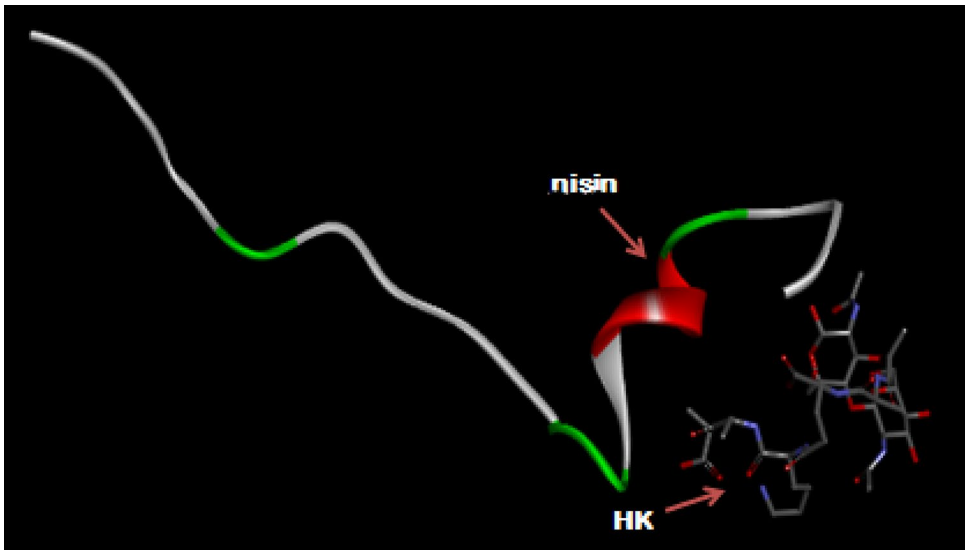

Fig. 8 Docking of the HPK with nisin using Z-dock. To examine protein–ligand interactions, models for ligand binding potency were predicted

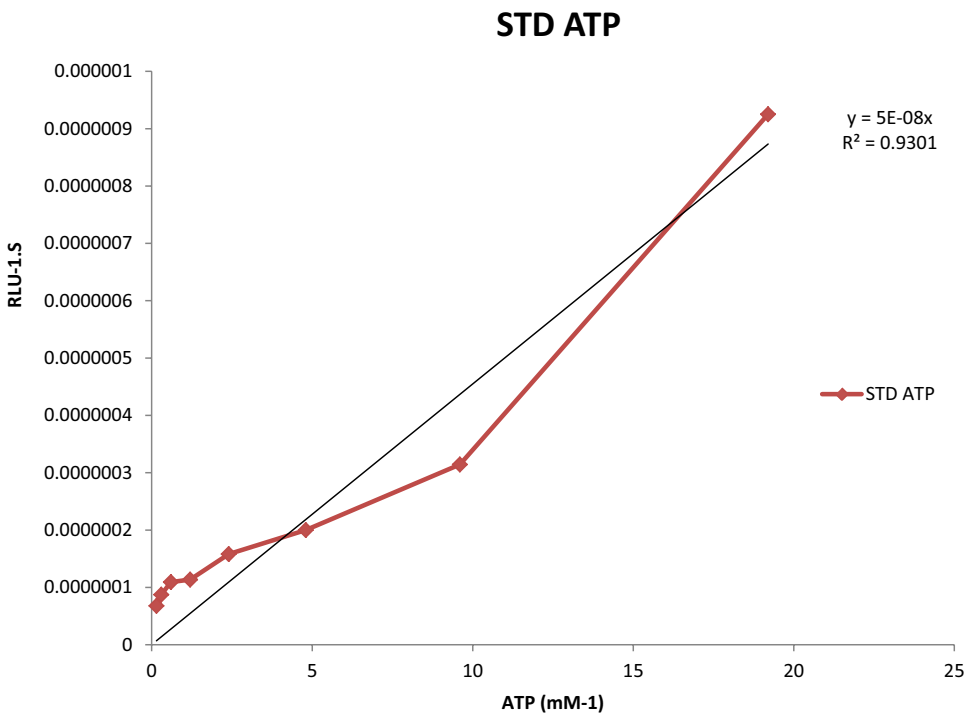

Fig. 9 Assay of NisK activity. A standard curve with different ATP concentrations

We selected the NisK and NisR proteins for study, which play a vital role in nisin production. The environmental factors of NisK and NisR proteins were our main concern affecting the nisin production; therefore, we had to express two recombinant proteins and study their production characteristics and also their activity properties. Regulating gene and protein expression is dependent on the secondary structure of mRNA (Gaspar et al. 2013).

In this research, sequences of NisK and NisR were blasted in order to search for the protein with nearest sequence similarity. NisR has 100% identity with response regulator protein of *Lactococcus Lactis* and 62.56% identity with the response regulator transcription factor [*Streptococcus pseudopneumoniae*]. NisK has 100% identity with sensor-receptor histidine kinase NisK [*Lactococcus lactis*] and also the least identity with its histidine kinase sensor [*Streptococcus mitis*] (Data not shown).

The evolutionary history was inferred using the Neighbor-Joining method. The optimal tree of Nisk protein with the sum of branch length = 4.28740154 and branch length = 3.07248116 of NisR is shown. The percentage of replicate trees in which the associated taxa clustered together in the bootstrap test (1000 replicates) are shown next to the branches. The tree is drawn to scale, with branch lengths in the same units as those of the evolutionary distances used to infer the phylogenetic tree. The evolutionary distances were computed using the Poisson correction method and are in the units of the number of amino acid substitutions per site. This analysis involved 82 amino acid sequences. All ambiguous positions were removed for each sequence pair (pairwise deletion option).(Figure 2a, b in supplementary).

The chemical and physical characteristics of the NisK and NisR proteins were analyzed by ExPASy Prot Param software. The pI values of both proteins (pI > 5.15 for NisR and PI > 5.71 for NisK) were calculated. The instability indexes for NisK and NisR were 44.79 and 54.07, respectively, which classified them as stable proteins. Two indexes (RMSD and TM score) were applied in order to confirm the precision of the prepared models. The accuracy of the models were confirmed by TM scores of NisK (0.54 ± 0.15) and NisR (0.79 ± 0.09). Generally a TM-score above 0.5 demonstrates the accuracy of the model. C-score and Z-score were also used for demonstrating that it is trustworthy.

Upon studying the topology results, it was observed that the nisK protein at the two ends of C-terminal and N-terminal have no trans membrane domains. This protein has two predicted transmembrane helics. Because the NisK protein is a transmembrane protein, the expected number of amino acids in transmembrane helics was higher than 18 and according to this figure is approximately 44.20.

Codon optimization can be considered as one of the essential steps in designing synthetic genes. The desired genes were derived from *Lactococcus lactis* subsp. *lactis* and in order to enhance the production in *E. coli*, genes were optimized. The CAI index was calculated for *nisK*: 0.93 and *nisR*: 0.94. PET28a-nisR and pET32a-nisK constructed vectors and genes were transformed into DH5α host cells and after the proliferation of the plasmids and plasmid extraction, restriction enzymes were used to verify the presence of the genes followed by gel electrophoresis assay. Then the pET28a-nisR plasmid was transformed into *E. coli* BL21 (DE3) strain and the pET32a-nisK plasmid was transformed into BL21, but we encountered a failure because the gene was not expressed, so we had to shift to the host Rosetta-gami (DE3).

The expression condition of proteins was optimized. *E. coli* Rosetta host competent cells were prepared and pET32a-nisK was transformed and cultured in medium containing ampicillin (50 µg/ml). For protein expression, isopropyl β-D-1-thiogalactopyranoside (IPTG) was used as an inducer with a final concentration of 1 mmol/l, incubating for 7 h at 37 °C. Simultaneously, pET28a-nisR was transformed into *E. coli* BL21 strain with kanamycin (50 µg/ml) and in order to decrease the inclusion bodies during expression, the induction was done by 0.5 mmol/l IPTG and was incubated overnight at 28 °C, followed by measuring their concentration. We optimized the protein expression to obtain both proteins and after purification and confirmation by SDS-PAGE, their concentrations were measured at approximately 400–500 mg/l. By western blotting, the NisK and NisR proteins were identified and their sizes also were confirmed.

Two methods of dialysis and rapid dilution were used concurrently to avoid the reduction of protein concentration and to prevent losing protein during dialysis and also to enhance the speed and the quality of the protein. By using this method, our protein concentrations somewhat was reduced.

One of the major factors affecting gene and protein expression is the secondary structure of mRNA (Gaspar et al. 2013). The results revealed that the stability of the mRNA was good enough to be maintained in the host. Results demonstrated that the folding free energies related to the 5′-untranscribed region were higher in comparison to the other regions and no hairpin could be seen in the 5′ region of the mRNAs in both genes. Thus, it can be expected that the protein expression and also the half-life of the proteins will be enhanced and will be at a profitable amount.

The results obtained from the CD analysis and from the prediction methods were in agreement, specifically in the predicted numbers of random coils and beta-sheets. Therefore, the NisR protein contains more than 45% alpha-helix and beta-sheet and is categorized into the family of proteins which own random coil more than any other protein structure.

In this study, It was important for us to determine the secondary structure (alpha helix, beta sheet and turn percentage) and tertiary structure of the NisK and NisR proteins. After the production of recombinant proteins, the secondary structure was also studied by CD spectroscopy. The comparison of the obtained data from bioinformatics and CD analysis revealed that not much change occurred in the structure of NisK and NisR proteins.

For protein molecular functions, the three-dimensional (3D) structure details were of major importance in providing intuitions. By using I-TASSER online software, three-dimensional models of the NisK and NisR proteins were generated along with their C-Score. Five NisK models were generated with the following C-scores: − 1.45, − 1.75, − 2.16, − 3.15, − 3.32, and five NisR models were generated with the following C-scores: − 0.57, − 1.50, − 2.08, − 3.18, − 2.88. Model 1 was selected for further analysis as it had the highest C-Score. models, model 1 has selected for further analysis as it contained the highest C-Score. Energy minimization resulted from analysis of 3D structural stability of the proteins using Swiss-Pdb Viewer.

One of the delicate and analytical tools used for detecting ATP consumption is calculating the amount of light produced by luciferase, which is done by using the Sirius tube luminometer (Berthold Detection System, Germany). Through this method, the activity assay of the NisK enzyme was measured. Several HPKs are able to act as phosphatases and cause signaling, because HPKs are capable of transferring a phosphoryl group from ATP to a histidine residue, followed by transportation of an aspartate to an RR.

The results demonstrated that this enzyme can separate phosphoryl group. The data showed that recombinant proteins NisK have well protein folding and structure and the proper function.

Acknowledgments The authors are grateful to Dr. A.M Latifi and Dr. S. Hossein Khani for their support of this research. This study was supported by the Baqiyatallah University of Medical Sciences and Applied Biotechnology Research Center.

Funding No funding supporter.

Compliance with ethical standards

Conflict of interest The authors declare that they have no conflict of interest.

Informed consent N/A.

Research involving human participants and/or animals N/A.

References

Chatterjee C, Paul M, Xie L, Van Der Donk WA (2005) Biosynthesis and mode of action of lantibiotics. Chem Rev 105:633–684

Cheung J, Hendrickson WA (2010) Sensor domains of two-component regulatory systems. Curr Opin Microbiol 13:116–123

Field D, Cotter PD, Hill C, Ross RP (2015) Bioengineering lantibiotics for therapeutic success. Front Microbiol 6:1363

Garnier J, Gibrat JF, Robson B (1996) GOR method for predicting protein secondary structure from amino acid sequence. Methods in enzymology. Elsevier, Amsterdam, pp 540–553

Gaspar P, Moura G, Santos MA, Oliveira JL (2013) mRNA secondary structure optimization using a correlated stem–loop prediction. Nucleic Acids Res 41(6):e73

Gasteiger E, Hoogland C, Gattiker A, Wilkins MR, Appel RD, Bairoch A (2005) Protein identification and analysis tools on the ExPASy server. The proteomics protocols handbook. Springer, New York, pp 571–607

Gharsallaoui A, Oulahal N, Joly C, Degraeve P (2016) Nisin as a food preservative: part 1: physicochemical properties, antimicrobial activity, and main uses. Crit Rev Food Sci Nutr 56(8):1262–1274

Grote A, Hiller K, Scheer M, Münch R, Nörtemann B, Hempel DC, Jahn D (2005) JCat: a novel tool to adapt codon usage of a target gene to its potential expression host. Nucleic Acids Res 33:W526–W531

Kamarajan P et al (2015) Nisin ZP, a bacteriocin and food preservative, inhibits head and neck cancer tumorigenesis and prolongs survival. PLoS ONE 10(7):e0131008

Kim W, Hall R, Dunn N (1998) Improving nisin production by increasing nisin immunity/resistance genes in the producer organism *Lactococcus lactis*. Appl Microbiol Biotechnol 50:429–433

Kuipers OP, Beerthuyzen MM, de Ruyter PG, Luesink EJ, de Vos WM (1995) Autoregulation of nisin biosynthesis in *Lactococcus lactis* by signal transduction. J Biol Chem 270:27299–27304

Mascher T, Helmann JD, Unden G (2006) Stimulus perception in bacterial signal-transducing histidine kinases. Microbiol Mol Biol Rev 70(4):910–938

Möller S, Croning MD, Apweiler R (2001) Evaluation of methods for the prediction of membrane spanning regions. Bioinformatics 17(7):646–653. https://doi.org/10.1093/bioinformatics/17.7.646

Mortazavi M, Hosseinkhani S (2011) Design of thermostable luciferases through arginine saturation in solvent-exposed loops protein engineering. Des Select 24:893–903

Reinelt S, Hofmann E, Gerharz T, Bott M, Madden DR (2003) The structure of the periplasmic ligand-binding domain of the sensor kinase CitA reveals the first extracellular PAS domain. J Biol Chem 278:39189–39196

Rostami A, Goshadrou F, Langroudi RP, Bathaie SZ, Riazi A, Amani J, Ahmadian G (2016) Design and expression of a chimeric vaccine candidate for avian necrotic enteritis protein engineering. Des Select 30:39–45

Sambrook J, Fritsch EF, Maniatis T (1989) Molecular cloning: a laboratory manual. Cold spring harbor laboratory press, New York

Schaller GE, Shiu S-H, Armitage JP (2011) Two-component systems and their co-option for eukaryotic signal transduction. Curr Biol 21:R320–R330

Tafreshi NK, Sadeghizadeh M, Emamzadeh R, Ranjbar B, Naderi-Manesh H, Hosseinkhani S (2008) Site-directed mutagenesis of firefly luciferase: implication of conserved residue (s) in bioluminescence emission spectra among firefly luciferases. Biochem J 412(1):27–33

West AH, Stock AM (2001) Histidine kinases and response regulator proteins in two-component signaling systems. Trends Biochem Sci 26:369–376

Wu J, Hu S, Cao L (2007) Therapeutic effect of nisin Z on subclinical mastitis in lactating cows. Antimicrob Agents Chemother 51:3131–3135

Wuichet K, Cantwell BJ, Zhulin IB (2010) Evolution and phyletic distribution of two-component signal transduction systems. Curr Opin Microbiol 13:219–225

Zhang Y (2008) I-TASSER server for protein 3D structure prediction. BMC Bioinform 9(1):40

Zhang Q, Yu Y, Vélasquez JE, Van Der Donk WA (2012) Evolution of lanthipeptidesynthetases. Proc Natl Acad Sci 109:18361–18366

Zuker M (2003) Mfold web server for nucleic acid folding and hybridization prediction. Nucleic Acids Res 31:3406–3415